ELSEVIER International Journal of Mass Spectrometry and Ion Processes 136 (1994) 167–180

Electrospray and Taylor-Cone theory, Dole's beam of macromolecules at last?

Matthias S. Wilm*, Matthias Mann

Protein & Peptide Group, European Molecular Biology Laboratory, Meyerhofstr. 1, D-69012 Heidelberg, Germany

Received 13 March 1994; accepted 14 June 1994

Abstract

A theoretical description of the electrostatic dispersion in electrospray is presented. The theory predicts the size of the zone at the tip of the Taylor Cone from which the liquid is ejected. To minimize this emission zone a modified electrospray ion source, the micro electrospray, has been constructed. With this ion source the size of the droplets is in the 200 nm range or below. The spray is very stable so that aqueous solutions can be dispersed in negative or positive mode without any assistance. The micro electrospray ion source is very efficient in the use of the applied amount of sample. Its flow rate of less than 25 nl/min makes MS–MS investigations on 0.5 μl of sample possible. An overall transmission coefficient of 8×10^{-4} for a peptide from the solution state to the detector has been measured.

Keywords: Electrospray; Electrospray theory; MS–MS; Peptides; Proteins; Taylor Cone

1. Introduction

Electrospray is one of the most versatile ionization techniques for the investigation of macromolecules. It was introduced in 1984 by Yamashita and Fenn and Aleksandrov et al. quasi simultaneously [1–3]. Already in 1968 Dole had proposed to use electrospray as a means to generate ions of macromolecules [4]. However, it was only in 1988 that Fenn and co-workers reported convincing experimental results for large molecules (poly(ethylene) glycols) up to 17 500 u [5] and proteins up to 40 000 u [6]). Today, Electrospray Mass Spectrometry (ESMS) is a widely used technique in biological, biochemical, pharmaceutical and medical research.

Electrospray ion sources spray fluid electrostatically out of a capillary with an inner diameter of typically 100 μm at a flow rate of 1–10 μl/min [7]. This way of operating an electrospray source leads to droplets with an initial diameter of more than 1 μm [7]. For an analyte concentration of 500 fmol μl^{-1} a sphere with a diameter of 1 μm contains more than 150 000 analyte molecules. So, how are single ions generated? For the generation of *small* ions Thomson and Iribarne proposed the field evaporation mechanism [8]. In this model, ions are field emitted from small, highly charged droplets produced by Coulomb explosions from the initially sprayed, larger droplets.

* Corresponding author.

0168-1176/94/$07.00 © 1994 Elsevier Science B.V. All rights reserved
SSDI 0168-1176(94)04024-2

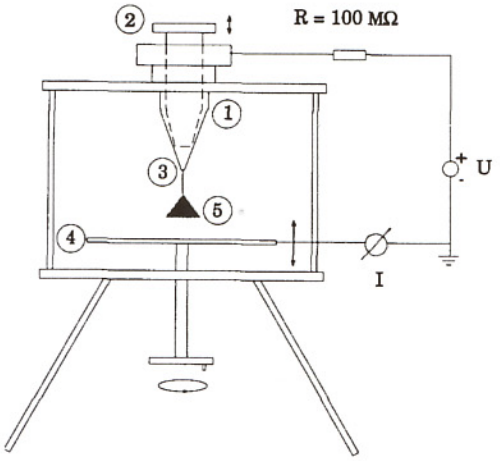

Fig. 1. Schematic overview of the experimental electrospray set-up. The fluid is filled into the reservoir (1). The flow resistance towards the nozzle (3) can be regulated through the height of the plunger (2) in the reservoir. The metal nozzle (3), through which the fluid is sprayed, has an inner diameter of 250 μm. The distance between the nozzle (3) and the ground plate (4) can be varied. During the experiments the fluid surface and the spray (5) were observed with a stereo microscope (Leica, type: wild M3B. magnification factor 6.4–40). The spray was initiated by applying positive voltage to the reservoir.

Fenn applied this mechanism to macromolecules [9, 10]. He proposed that a charged part of a molecule penetrates the surface of a droplet. The coulomb repulsion between this part of the molecule and the droplet surface would pull the entire molecule out of the droplet. An alternative proposal is based on the original idea of Dole [4,11,12]. The highly charged droplets produced by the electrospray source shrink by solvent evaporation. By repetitive Coulomb explosions nanometer sized droplets are generated which contain only one macromolecule. The solvent molecules evaporate leaving the macromolecules as ions. In this model the ionization is a passive process whereas in the ionization mechanism proposed by Fenn the macromolecule plays an active role [13].

In this paper we develop a theoretical description of the electrospray process. The model is based on the original Taylor Cone theory [14]. Our objects were (a) to derive a formula which describes the onset voltage of the spray quantitatively, (b) to quantify the diameter of the zone at the tip of the Taylor Cone which ejects the liquid and (c) to gain an insight into the ionization process. The theoretical model provided guidance for the construction of a more efficient ionization source, a source which we call the "micro electrospray" source [15]. Some experimental results with this ion source on a triple quadrupole mass spectrometer are shown which support the theoretical results.

2. Experimental

Basic characteristics of the electrospray source were measured by the experimental set-up shown in Fig. 1.

For the experiments with the bench-top electrospray fluid is filled into a reservoir (1). By adjusting the flow resistance with a plunger (2) the fluid just reaches the downward pointing nozzle (3) without leaking out. When a sufficient voltage is applied to the nozzle the fluid is dispersed electrostatically. The process can be followed by measuring the electrical current between the nozzle and the ground plate (4) and by observing the spray through a microscope. The flat counterelectrode (4) does not have the shape of an equipotential plane as described by Eq. (13). This limits the correspondence between the experimental set-up and the theoretical description, but the trend of the experimental results should not be affected.

For the investigation of the current/voltage characteristics acetone was filled into the reservoir. The distance between the nozzle and the ground plate was adjusted to 1 cm. Between 2.5 kV and 3.6 kV the fluid was dispersed from a stable, central cone. Under these conditions the current/voltage relationship was recorded for four different flow resistances. The flow resistance could be coarsely regulated by changing the height of the plunger in the reservoir.

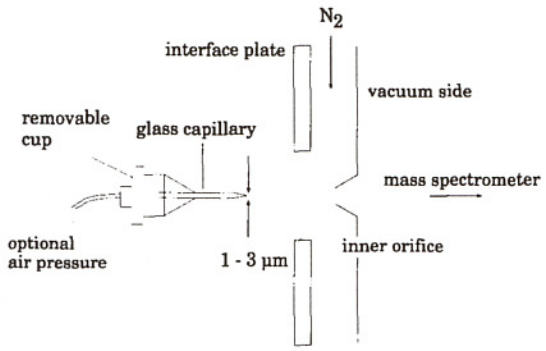

Fig. 2. The micro electrospray source mounted on an API-III electrospray mass spectrometer. The capillary has an inner diameter of 1 to 3 μm at its tip. It is mounted at a distance of 1 to 2 mm in front of the inner orifice of the mass spectrometer. 0.5 to 1 μl of an analyte solution is filled into the capillary and sprayed directly from the tip of the capillary towards the orifice. No assistance such as nebulizer, sheath flow or SF_6 gas is employed. Air pressure of less than 1 bar can be applied in cases where salt loaded aqueous solutions with a high viscosity are sprayed. This was not the case in the experiments described here.

For the investigation of the dependence of the threshold voltage U_T on the distance between the nozzle and the ground plate acetone was filled into the reservoir and, for a given distance, the applied voltage was slowly increased until the Taylor Cone formed and the spray started.

Measurements of the relationship between the flow rate and the size of the droplets was done by spraying a 6.5×10^{-5} mol l^{-1} acetone solution of rhodamine G on a metal target. The distance between the nozzle and the target was 1 cm. The spray was operated at 2.8 kV. The size of the rhodamine particles on the target was measured under a microscope.

Additionally a "micro electrospray" ion source has been constructed. Its properties were investigated with a triple quadrupole mass spectrometer (API III, Perkin-Elmer Sciex Instruments, Thornhill, Canada) (see Fig. 2).

The liquid is sprayed from the tip of a gold coated borosilicate glass capillary with an orifice of 1–3 μm. The tip of the capillary has been formed with a micro pipette puller (model P-87 Puller, Sutter Instrument Company, Novato, CA, USA). This instrument allows one to pull the tips quickly and reproducibly.

The capillary tip of the micro electrospray source is centered at a distance of 1–2 mm from the inner orifice of the mass spectrometer (i.e. of the vacuum interface). A voltage of about 600 V is applied to the capillary, 100 V to the interface plate and 80 V to the inner orifice. Evaporation of the droplets is achieved by a counter flow of heated nitrogen (99.999% pure, flow rate of 0.2–0.6 l min^{-1}, 58°C) in front of the orifice. All spectra were obtained by scanning the first quadrupole Q_1 over the applicable m/z range. The second quadrupole Q_3 was left in the RF-only mode. Air pressure can be applied to ensure a sufficient liquid flow through the small capillary in case of salt loaded aqueous liquids with a high viscosity.

The total ion transmission of the experimental set-up was measured with a synthetic peptide (mass 1875.1 u). The peptide was dissolved in 1% formic acid in aqueous methanol (1 : 1) and 1 μl of a 0.5 pmol μl^{-1} solution was applied to the capillary and sprayed into the mass spectrometer. The $(M + 2H)^{2+}$ was recorded until no fluid remained in the capillary. The total number of detected ions in comparison to the number of peptide molecules filled into the capillary yields the total transmission.

2.1. Chemicals

Rhodamine G was purchased from Sigma (Sigma Chemie GmbH, Deisenhofen, Germany). Acetone was of HPLC-grade from Labscan (Labscan Ltd. Stillorgan, Co., Dublin, Ireland). The peptide used was synthesized in our group on an Applied Biosystems (ABI) 431 A synthesizer (Applied Biosystems, Weiterstadt, Germany) using Fmoc chemistry and purified by reverse phase high performance

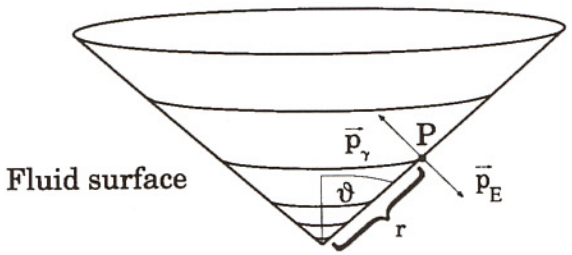

Fig. 3. The liquid Taylor Cone, ϑ is the cone angle, p_γ the pressure caused by the surface tension and p_E the pressure caused by the electrical field on the surface of the cone. r is the distance of the point P from the tip of the cone.

liquid chromatography (HPLC) (sequence: MDMSKDESVDYVPMLD, UIPAC one letter code for amino acids, average mass 1875.1 u).

3. Results and discussion

First the static case in which no fluid is dispersed is described to establish the physical model. In a second step this model is applied to the spraying mode.

3.1. The electrical field around a conical and conducting surface

As we are considering the static case a conducting surface can be assumed. Therefore, the electrical field is orthogonal to the surface. The main forces which act on the surface are the surface tension and the electrostatic force [16]. (Gravitational forces are neglected in this description. However, they do play a role when the electrostatic force just equilibrates the surface tension.) The electrostatic force pulls the liquid out of the nozzle towards the ground plate. The surface tension retracts it to minimize the surface area.

$$p_\gamma = \gamma\kappa \tag{1}$$

where p_γ is the pressure derived from the surface tension, γ is the surface tension and κ is the curvature of the surface

$$p_E = 0.5\epsilon_0 E^2 \tag{2}$$

where p_E is the electrostatic pressure and E is the electrical field at the surface.

The electrostatic pressure p_E can be calculated when the Poisson equation for a conical equipotential plane is solved. The retracting force p_γ is determined by the curvature of the surface. As shown in the Appendix the following equations for the two pressures can be derived in the chosen spherical coordinate system (r, ϕ, θ).

$$p_\gamma = \gamma \frac{\cos\vartheta}{(1-\cos^2\vartheta)} \frac{1}{r} \tag{3}$$

where ϑ is the liquid cone angle (see Fig. 3),

$$P_E = \tfrac{1}{2}\epsilon_0 \phi_0^2 r^{2(n-1)} \left[\frac{\partial}{\partial\theta} P_n(\cos\theta)\right]^2 \tag{4}$$

where ϕ_0 is the constant of the electrical potential, P_n is the Legendre Polynom of the degree n and n is a parameter describing the radius dependence of the potential ϕ.

3.2. The Taylor Cone as the solution for the static equilibrium

In the static case the pressures due to the electrostatic force and due to the surface tension must be equal for all points on the surface of the cone, i.e. $p_E = p_\gamma$. Therefore the dependence on r must be the same for both pressures. This condition is only met by $n = 0.5$. The condition that the electric field is orthogonal to the surface can only be satisfied by $P_{1/2}(\cos\theta) = 0$ (see Appendix, Eq. (12)) which in turn requires $\theta_P = 180° - \vartheta = 130.7°$ [16].

This description of the liquid cone considering only the surface tension and the electrostatic force results in the classical Taylor Cone formula for the electrical potential.

$$\phi(r,\theta) = \phi_0 r^{0.5} P_{1/2}(\cos\theta)$$

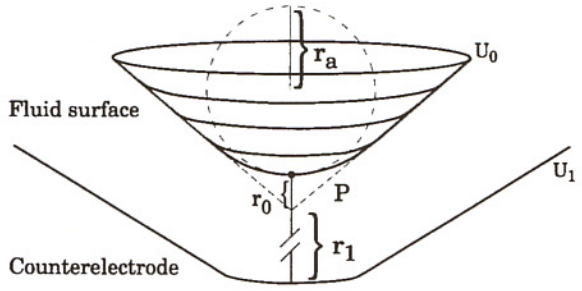

Fig. 4. The fluid surface with a voltage setting below the threshold for Taylor cone generation. The liquid is pulled out of the nozzle forming half an ellipsoid. The state is static. No fluid is dispersed. $U_1 - U_0$ is the applied voltage U_a. Note that the distance r_1 between the tip of the cone and the counter electrode is much larger than the distance r_0 between the apex point of the ellipsoid P and the cone tip ($r_1 \gg r_0$). r_a is the radius of curvature of the best fitting circle at the tip of the cone.

with the condition that the liquid cone angle ϑ equals 49.3°. Note that it is only in the static case that the angle is fixed to 49.3°. In the dynamic case when fluid is sprayed the angle decreases somewhat with increasing flow rate [17]. The singularity of the electrical potential at the apex of the cone indicates that the theoretical description is a model description of a physical phenomenon.

3.3. The creation of the Taylor Cone from an elliptically shaped fluid cone

Fig. 4 shows the state before the Taylor Cone is formed and, thus, before the fluid is sprayed. The aim of the following discussion is to understand the observed sudden change of the ellipsoid into a pointed cone when the voltage exceeds the threshold. It will lead to a formula describing the variation of the threshold voltage of the spray as a function of the distance r_1 to the plane of ground potential.

The electrical potential is assumed to contain the Taylor Cone potential and a perturbation term [16]. With this assumption it can be assured that the shape of the ellipsoid approximates the shape of the Taylor cone. The r dependence of the perturbation term must be $r^{2/3}$ (see Appendix Eq. 10 with $n_1 = 1/2$).

$$\phi(r,\theta) = \phi_0(r^{0.5} - a^2 r^{-1.5}) P_{1/2}(\cos\theta) \qquad (5)$$

The parameter a will be used to fit the shape of the ellipsoid to the geometry of the Taylor Cone [16]. With this electrical potential the electrostatic pressure on the apex point of the elliptic fluid cone can be calculated (see Appendix). The result is (see Eq. 16)

$$p_\gamma - p_E = 1/r_a(2\gamma - 2.68\epsilon_0 U_a^2 r_1^{-1}).$$

This equation describes the behavior of the liquid surface when a voltage U_a is applied to the fluid. When this voltage reaches the threshold voltage U_T the electrostatic pressure p_E equals the pressure p_γ due to the surface tension for every radius of curvature r_a of the tip of the ellipsoid. This is the moment when the surface rapidly changes its shape to become a pointed cone.

$$U_T = 0.863(\gamma r_1/\epsilon_0)^{0.5} \qquad (6)$$

This formula expresses the dependence of the threshold voltage on the distance to the counter electrode (see Fig. 4).

3.4. The emission radius for droplets from the spraying Taylor Cone

We extended the description of the static case to the dynamic one. This is certainly an approximation which is only strictly justified as long the experimental conditions are not too far from the static Taylor Cone. We assumed in the theoretical description that the surface of the liquid is an equipotential plane. This is not any longer true for a situation far from static equilibrium. Then there is a voltage drop over the liquid cone and the cone angle becomes smaller than 49.3° [17].

The aim in the following derivation was to find an expression for the size of the zone from which the liquid is ejected.

For high flow rates a jet of liquid emerges from the tip of the Taylor Cone which

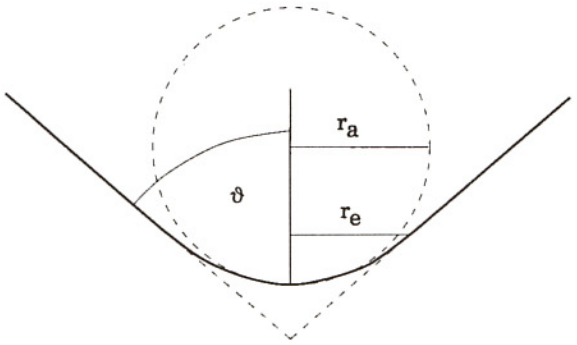

Fig. 5. The cone, snap shot between the emission of two droplets. r_e is the radius of the zone at the tip of the Taylor Cone, which emits droplets, i.e. the emission radius. r_a is the radius of curvature at the tip of the cone.

breaks up into a series of droplets. The lower the flow rate the shorter the jet. For very small flow rates a direct emission of droplets may be reached. In this case the emission diameter corresponds exactly to the diameter of the droplets. In general the droplet size is larger than the emission diameter, but the smaller the flow rate the better the correspondence between the emission diameter and the droplet size should be (see Fig. 8).

Fig. 5 shows the geometry of the spraying cone. To describe the fluid dynamics of the spray the Bernoulli Equation must be solved [18].

$$0.5\rho v^2 + p = 0 \tag{7}$$

where v is the velocity of the fluid, ρ is the density of the fluid and p is the pressure.

The first term can be related to the flow rate $\mathrm{d}V/\mathrm{d}t$ using the geometry shown in Fig. 5.

$$v = \frac{\mathrm{d}V/\mathrm{d}t}{\pi r_e^2}$$

The pressure at the apex point can be calculated as follows:

$$p = p_\gamma - p_E = 2\gamma/r_a - 0.5\epsilon_0 E^2$$

where U_a is the applied voltage and U_T the threshold voltage.

With $E = \mathrm{d}U_a$ (see Appendix, Eq. (15)) and the condition that the pressure due to the surface tension equals the electrostatic pressure just when the threshold voltage is reached, i.e. $2\gamma/r_a = 0.5\epsilon_0 E_T^2 = 0.5\epsilon_0\gamma^2 U_T^2$, we find an expression for the pressure when the applied voltage exceeds the threshold voltage.

$$p = \frac{2\gamma}{r_a}\left[1 - \left(\frac{U_a}{U_T}\right)^2\right] \tag{8}$$

The results for v and p can be used in the Bernoulli Equation and r_a can be replaced by an expression in r_e (see Appendix, Eq. 17). A formula results which describes the size of the zone at the tip of the Taylor Cone from which droplets are ejected:

$$r_e = \left(\frac{\rho}{4\pi^2\gamma\tan\left(\frac{\pi}{2} - \vartheta\right)\left[\left(\frac{U_a}{U_T}\right)^2 - 1\right]}\right)^{1/3} \times (\mathrm{d}V/\mathrm{d}t)^{2/3} \tag{9}$$

with r_e the radius of the emission region for droplets at the tip of the Taylor Cone (see Fig. 5), γ the surface tension of the liquid, ϑ the liquid cone angle (for the classical Taylor Cone model $\vartheta = 49.3°$), ρ the density of the liquid, U_T the threshold voltage, U_a the applied voltage and $\mathrm{d}V/\mathrm{d}t$ the flow rate.

This formula relates the flow rate to the emission diameter for droplets emerging from the tip of the Taylor Cone. The emission diameter r_e is proportional to the 2/3 power of the flow rate $\mathrm{d}V/\mathrm{d}t$.

3.5. The current/voltage characteristics of the spray

The calculation of the $I-U$ characteristics from the theoretical description of the electrospray process can not be made without making assumptions about the charge density on the surface of the droplets as a function of the applied voltage. Increasing the applied voltage

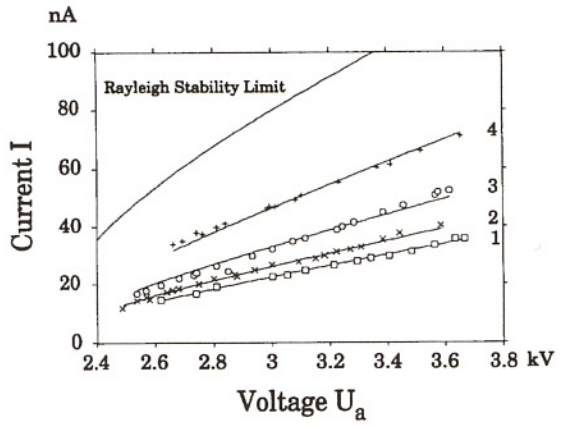

Fig. 6. The current/voltage characteristics of the electrospray using the apparatus of Fig. 1 at four different flow resistances. Acetone is sprayed. The flow resistance in the reservoir was highest for the measurement 1 and lowest for the measurement 4. The charge transported by the droplets stays below the maximum transportable charge, i.e. when all droplets are charged to the Rayleigh stability limit (see Eq. 19). The lines are fitted according to Eq. (18) (see text).

means increasing the field density at the tip of the Taylor Cone. On the other hand increasing the voltage means increasing the size of the emission region because the flow rate becomes larger caused by the larger force pulling on the fluid (see Eqs. 8, 9). The increased size of the emission region reduces the density of the electrical field. It turns out that the assumption of a constant electrical field density at the tip of the cone throughout the experiment can explain the observed results to a first approximation (see Fig. 6). Therefore we assume a constant surface charge density c on the emitted droplets. The following relationship between the current and the voltage can be deduced (see appendix, Eq. 18):

$$I = 6\left(\frac{\pi^2}{\rho}\right)^{2/5} \frac{c}{R_f^{1/5}} \left(\gamma \tan\left(\frac{\pi}{2} - \vartheta\right)\right)^{3/5} \times \left\{\left(\frac{U_a}{U_T}\right)^2 - 1\right\}^{3/5}$$

with R_f the overall flow resistance.

The surface charge density on the droplets is limited by the Rayleigh stability criterion [14]. The maximum electrical current, i.e. the current which would flow if all droplets were charged to the Rayleigh limit, can be calculated within this model (see Appendix, Eq. 19). The comparison between the measured current and the maximum possible current gives an estimate of the degree to which the droplets are charged.

3.6. Experimental confirmation of the theoretical model

For the characterization of the electrospray in general the current/voltage characteristics of the spray were investigated. The reservoir of the experimental electrospray set-up (see Fig. 1) was filled with acetone. No specific flow rate was enforced by a pump, no additional force was applied to the liquid. With a slow increase of the applied voltage U_a the elliptic shape of the fluid surface is elongated by the electrostatic forces between the ground plate and the fluid. At a certain threshold voltage U_T the surface suddenly changes its shape into a pointed cone. The Taylor Cone, and the spray commences (see Fig. 1). The fluid is dispersed from the tip of the cone in the form of a narrow jet. After a flight path of about one to two millimeters the jet spreads into a fine mist of droplets. Further downstream the droplets become so small that they are no longer visible. When spraying highly conducting liquids with low flow rates the narrow jet becomes very short so that the conical region of dispersed droplets emerges quasi directly from the liquid cone [17]. The droplets which are emitted from the Taylor Cone shrink by solvent evaporation. The shrinking, highly charged droplets may reach a limit where the Coulomb repulsion exceeds the surface tension (Rayleigh stability limit). This would lead to an electro-hydrodynamic instability, either of the whole droplet or of a localized region [11, 19]. Each droplet would

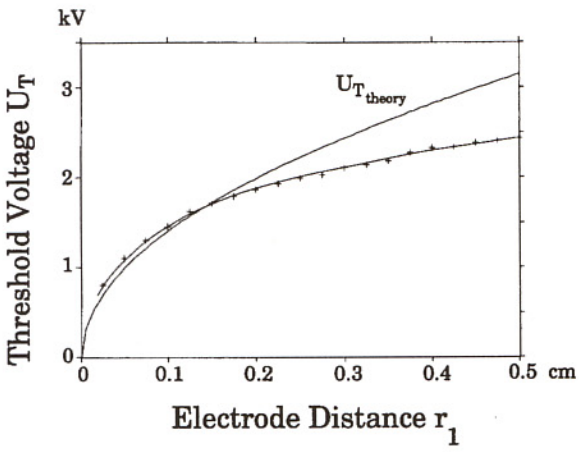

Fig. 7. The variation of the threshold-voltage U_T for the creation of the Taylor cone with electrode distance. The threshold voltage depends on the distance of the nozzle to its counter electrode, the ground plate (see Fig. 1, 6). The measured voltages are shown in comparison to the theoretical values (see Eq. (6)).

give rise to several smaller ones. The electrohydrodynamic instability of the sprayed droplets is a possible explanation for the sudden spread of the jet into a mist of smaller droplets. An alternative explanation would be the space charge repulsion of droplets which are rapidly slowed down in air.

The charged droplets transport a current between the nozzle and the ground plate. Fig. 6 shows the current/voltage characteristics of the spray for different flow resistances. It is remarkable that the current/voltage characteristics show a virtually linear behavior in the stable spray region. This is in contrast to other experiments using pumped flow [17]. With the assumption that the surface charge density stays constant throughout an experiment the following relationship was deduced: $I \propto (1/R_f^{1/5}) \cdot [(U_a/U_T)^2 - 1]^{3/5}$ (see Eq. 18). The curves shown in Fig. 6 correspond to functions of the type $a_i \cdot [(U_a/U_T)^2 - 1]^{3/5}$, $i = 1, \ldots, 4$, with $U_T = 2.22\,\text{kV}$. The smaller the flow resistance, R_f, adjusted coarsely with the plunger, the higher the value of a_i ($a_1 = 25.4\,\text{nA}$, $a_2 = 29.4\,\text{nA}$, $a_3 = 37.1\,\text{nA}$, $a_4 = 52.3\,\text{nA}$). The charge of each droplet stayed under 70% of the maximum charge at the Rayleigh stability level which agrees well with reported observations of the maximum charge carried by the droplets [20].

The sudden onset of the Taylor Cone is characteristic for a fluid surface under the influence of an electrical field [14]. Fig. 7 shows the dependence of the threshold voltage on the distance between the metal nozzle and the ground plate (see Fig. 1). For small electrode distances ($r_1 \leq 400 \cdot r_e$, r_1 electrode distance, r_e emission radius for the droplets) a surprisingly good correspondence is obtained between theory and experiment in view of the fact that no adjustable parameters were used.

The flow rate determines the size of the emission region for droplets at the tip of the Taylor Cone as indicated by Eq. (9). The size of the sprayed droplets could not be measured directly with our experimental set-up. Therefore, a highly concentrated rhodamine G solution was sprayed onto a metal target and the size of the collected rhodamine particles was measured. The rhodamine precipitates in the sprayed droplets after some acetone has evaporated because the solution was saturated. Therefore, the rhodamine particles on the target should roughly represent the size of the emitted droplets.

Fig. 8 indicates that the size of the emitted droplets can be reduced by a reduction of the flow rate and that Eq. (9) gives a good absolute estimate of the size of the droplets.

3.7. The micro electrospray as an efficient ion source for electrospray mass spectrometry

In large droplets much of the liquid volume may not be available for the desorption of large molecular ions. A smaller initial volume may therefore increase the desorption/ionization efficiency. Following the concept described by Eq. (9) a micro electrospray source was constructed. Our reasoning was that small capillaries would allow small flow

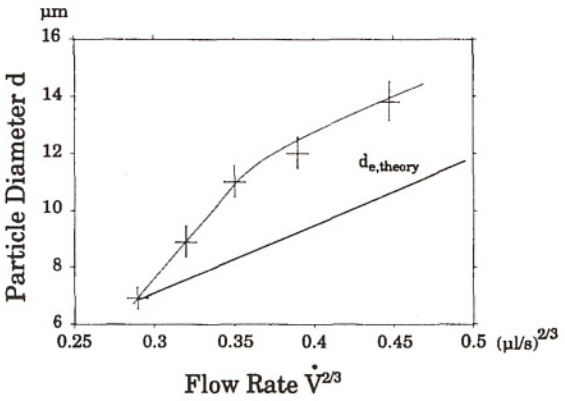

Fig. 8. Dependence of rhodamine particle size on the flow rate of the spray. A solution of rhodamine G in acetone was sprayed onto a target with the bench-top electrospray and the size of the rhodamine particles was measured. d_e is the calculated diameter of the emission zone of the droplets (see Eq. (9) with $U_T = 2.22\,kV$ and $U_a = 2.8\,kV$).

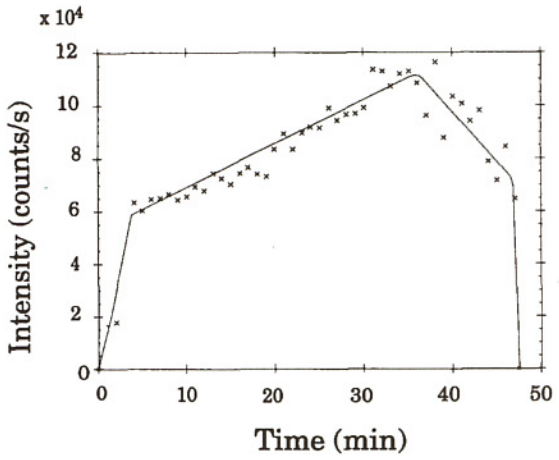

Fig. 9. Peptide ion intensity measured as a function of time on a Sciex API electrospray mass spectrometer equipped with a micro electrospray ion source. The capillary was filled with 1 µl of a 0.5 pmol µl^{-1} peptide solution. No sheath flow or assistance gas was employed. The peptide was observed in the doubly charged ionization state ($[M + 2H]^{2+}$).

rates in a stable manner. The electrospray ion source on a Sciex triple quadrupole was replaced by a pointed, gold coated glass capillary with an opening diameter at the tip of 1–3 µm and a length of 2–3 cm (see Fig. 2).

The micro electrospray ion source was operated between 580 and 800 V. This is well below the 3–5 kV usually applied to conventional ion sources. The strength of the electrical field E at the tip of the capillary is the decisive parameter for the spraying process and must be the same for all sizes of capillaries (see Eqs. 2, 6). The sharpness of the pointed capillary and the small distance from the tip to the counter electrode (1–2 mm) allowed the reduction in the applied voltage (see Fig. 7) while keeping the same field strength.

For measuring the ionization efficiency of the micro electrospray source 1 µl of a 0.5 pmol µl^{-1} solution was applied to the capillary and sprayed into the mass spectrometer.

Fig. 9 shows the peptide ion intensity over time. The increase in signal intensity during the experiment may be due to an increase in the concentration of the peptide in the sprayed solution because solvent evaporates slowly from the rear of the capillary (see Fig. 2). With 1 µl solution the spray lasted for ca. 45 minutes. From this measurement the mean spray rate can be calculated to be $< 25\,nl\,min^{-1}$.

By measuring the ion counts for $(M + 2H)^{2+}$ at the detector and dividing it by the number of peptide molecules sprayed the overall efficiency can be calculated to be 8×10^{-4} when the quadrupole is adjusted to unit mass resolution. This means that 1 out of 1300 peptide molecules in the solution are detected. If we assume a combined loss of a factor of hundred due to the detection system and the transmission of the quadrupole then the desorption/ionization efficiency and transfer into the vacuum system must have an efficiency of about 10%. Conventional electrospray ion sources typically lose orders of magnitude more in these steps.

With a flow rate of $25\,nl\,min^{-1}$ the radius r_e of the zone which emits droplets from the tip of the Taylor Cone (see Fig. 5) can be calculated to be $r_e = 88\,nm$ (see Eq. (9) with $\rho = 896\,kg\,m^{-3}$, $\gamma = 0.03531\,N\,m^{-1}$ (water, methanol 1 : 1) [21], $U_T = 550\,V$, $U_a = 600\,V$, $dV/dt = 25\,nl\,min^{-1}$).

The capillary has an orifice of 1–3 μm. On that orifice a Taylor cone forms and only from the tip of this cone droplets are ejected (see Fig. 1). Therefore, an emission diameter of about 180 nm does not seem unrealistic. No Taylor Cone or plume could be observed at 40× magnification with a microscope, providing additional support for a small droplet size.

A sphere with a diameter of 180 nm with an analyte concentration 0.5 pmol μl^{-1} contains statistically less than one analyte molecule (0.86). The emitted droplets may be elliptically shaped so that their volume is larger than the volume of a sphere with the diameter of the emission region. But since similar transmission results can be obtained with a concentration of 0.05 pmol μl^{-1} it is clear that a complete separation of analyte molecules into different droplets can be achieved with the micro electrospray.

The micro electrospray is a more stable ion source than conventional sources. Aqueous solutions, even with a moderate salt load ($c_{NaCl} \leq 100$ mmol l^{-1}), can be sprayed in positive or negative mode.

Independently of our work Gale and Smith realized an electrospray ion source with a small spraying tip [22]. For the interface between a capillary electrophoresis and an electrospray mass spectrometer they needed a low flow electrospray ion source. They observed an improvement in sensitivity as well and speculate that it may have been caused by the generation of smaller droplets.

4. Conclusion

A theory had been developed on the static description of the equilibrium between two forces, the surface tension and the electrostatic attraction, on the surface of a fluid under the influence of a high electric field. It yields results which agree with our experimental data (see Fig. 7, Eq. 6). The extension of the description to the dynamic spraying mode results in a relationship between the size of the zone at the tip of the Taylor Cone which emits droplets and the flow rate (see Eq. 9, Fig. 8). Inspired by this correlation we built a modified electrospray source, called micro electrospray. With this ion source the desolvation and ionization efficiency of analyte molecules were increased significantly. On a Sciex API triple quadrupole instrument interfaced with the micro electrospray source an absolute ion transmission of 8×10^{-4} for a peptide from the solvated state to the detector was measured. This high transmission agrees well with the theoretical calculations which show that a virtually complete separation of the analyte molecules in individual droplets is achieved. This degree of separation may have implications for the models of the ionization process. An ion evaporation model may not be required to explain the generation of large molecules from these small droplets — a simple desolvation process may be sufficient. Nevertheless, the ion evaporation model can not be ruled out as a possible ionization mechanism for large molecules.

4.1. Outlook

The high stability of the source makes the electrospray investigation more independent of solvents and buffers in a sample. Substances that require special solvents might be better analyzable with this source.

The low flow rate of the micro electrospray has the major advantage that it increases the measurement time considerably. Thus, instrumental parameters, for instance the collision energy in MS/MS experiments, can be optimized using as little as 0.5 μl of solution.

It has been shown that during electrospray ionization non covalent interactions between molecules can be preserved. The proposed ionization process by which unsolvated ions are expelled from highly charged droplets via

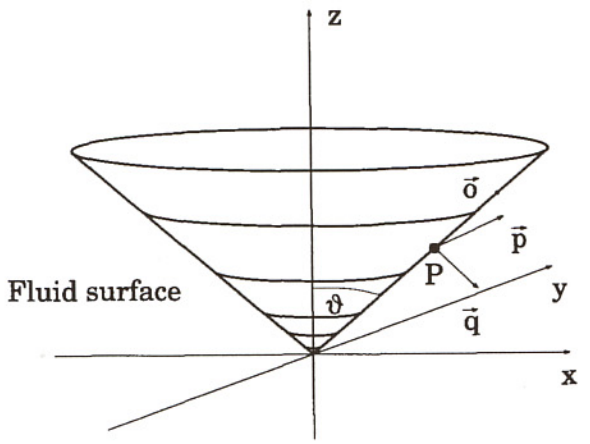

Fig. 10. Geometric representation of the Taylor Cone. Only the liquid cone is shown. The cone is rotationally symmetric around the z-axis and is characterized by the cone angle ϑ. The vectors $(\vec{o},\vec{p},\vec{q})$ describe an orthonormal system in the point P at the surface of the cone.

evaporation makes it difficult to understand how non covalent bounds can be preserved. These aspects are discussed in greater detail by R. Smith et al. [12]. They speculate that ion generation may occur from small clusters in the nanometer scale which contain only one analyte molecule (similar to Röllgen's proposal and to Dole's original ideas) [4, 11]. The micro electrospray seems to generate droplets in the 100 nm size range which fulfill the prerequisites of these speculations.

For the investigation of non covalent interactions with electrospray mass spectrometry the high degree of separation reduces the probability of unspecific clustering [12]. The reliability of this type of investigation may be improved considerably. Additionally, the high stability of the source facilitates the investigation. Aqueous solutions can be sprayed in negative or positive mode without any assistance.

Until now electrospray has been exclusively used for analytical purposes. Using the concept of micro electrospray it is relatively easy to arrange dozens of capillaries into a closely packed array to generate a very intense beam of macromolecules. Such a device could be suitable for using electrospray to generate macromolecular beams on a larger scale.

5. Appendix

5.1. The pressure caused by the surface tension

The surface O in Fig. 10 is characterized by:

$$O = \{(x,y,z)|z = f(x,y), f(x,y) = \cot\vartheta(x^2+y^2)^{1/2}\}$$

The point P and the orthonormal system $(\vec{o};\vec{p};\vec{q})$ are defined by:

$$P = (p_x; 0; \cot\vartheta \cdot p_x), \quad P \in 0$$

$$\vec{o} = (\sin\vartheta; 0; \cos\vartheta)$$

$$\vec{p} = (0; 1; 0)$$

$$\vec{q} = (\cot\vartheta; 0; -1)\frac{1}{(\cot^2\vartheta+1)^{1/2}}$$

With $Df = (\partial f/\partial x; \partial f/\partial y; \partial f/\partial z)$ we get the curvature of the surface in the point P as

$$\kappa_P = D[Df\vec{o}]\cdot\vec{o}|_P + D[Df\vec{p}]\cdot\vec{p}|_P = \cot\vartheta\frac{1}{p_x}$$

On the circle through P in a plane parallel to the x–y plane we have $\kappa = \kappa_P$ and $z = \cot\vartheta \cdot p_x$ and therefore

$$z\tan\vartheta = p_x = (x^2+y^2)^{1/2}$$

Replacing p_x in the equation for κ_p we get for κ

$$\kappa(x,y) = \cot\vartheta\frac{1}{(x^2+y^2)^{1/2}} = \frac{\cos\vartheta}{1-\cos^2\vartheta}\frac{1}{r}$$

Hence, the pressure caused by the surface tension on a rotationally symmetric cone with the liquid cone angle ϑ in the point $S(r,\phi,\vartheta)$ is:

$$p_\gamma = \gamma\frac{\cos\vartheta}{(1-\cos^2\vartheta)}\frac{1}{r} \tag{3}$$

where the symbols are as defined above.

5.2. The pressure caused by the electrostatic force

The surface of the cone is considered to be a conducting plane representing a certain electrical potential. The Poisson equation for the external, charge free space has to be solved:

$$\Delta\Phi = 0$$

The theoretical description does not contain any further boundary conditions. This means the cone has an "indefinite" extension into the z-direction. Because of the rotational symmetry around the z-axis ($\Phi = \Phi(r, \theta)$) the following equation holds:

$$\frac{1}{r^2}\left(\left[r^2\frac{\partial^2}{\partial r^2} + 2r\frac{\partial}{\partial r}\right] + \left[\frac{\partial^2}{\partial\theta^2} + \frac{\cos\theta}{\sin\theta}\frac{\partial}{\partial\theta}\right]\right)\Phi = 0$$

The equation can be solved independently for r and θ. With $\Phi = f(r)g(\theta)$ we get

$$\left(\left[r^2\frac{\partial^2}{\partial r^2} + 2r\frac{\partial}{\partial r}\right]f(r)\right)\frac{1}{f(r)}$$

$$+\left(\left[\frac{\partial^2}{\partial\theta^2} + \frac{\cos\theta}{\sin\theta}\frac{\partial}{\partial\theta}\right]g(\theta)\right)\frac{1}{g(\theta)} = 0$$

This differential equation allows the separation into r and θ.

$$\left(\left[r^2\frac{\partial^2}{\partial r^2} + 2r\frac{\partial}{\partial r}\right]f(r)\right)\frac{1}{f(r)} = c$$

$$c + \left(\left[\frac{\partial^2}{\partial\theta^2} + \frac{\cos\theta}{\sin\theta}\frac{\partial}{\partial\theta}\right]g(\theta)\right)\frac{1}{g(\theta)} = 0$$

solving the first differential equation for $f(r)$ with $f(r) = r^n$ we have

$$n(n+1) = c \qquad (10)$$

Using this result for c in the second differential equation we get a Legendre differential equation in $\cos\theta$.

$$(1 - \cos^2\theta)\frac{\partial^2}{\partial\cos\theta^2}g(\theta) - 2\cos\theta\frac{\partial}{\partial\cos\theta}g(\theta)$$

$$+n(n+1)\cdot g(\theta) = 0$$

$$\Rightarrow g(\cos\theta) = P_n(\cos\theta)$$

It follows that the electrical potential ϕ must fulfill:

$$\Phi(r, \cos\theta) = \Phi_0 \cdot r^n \cdot P_n(\cos\theta) \qquad (11)$$

Using the geometry of the cone we can calculate the electrical field $\boldsymbol{E}$ on the surface.

$$\vec{\boldsymbol{E}} = -\vec{\nabla}\phi$$

$$\vec{\nabla} = \frac{\partial}{\partial r}\vec{e}_r + \frac{1}{r\sin\theta}\frac{\partial}{\partial\varphi}\vec{e}_\varphi + \frac{1}{r}\frac{\partial}{\partial\theta}\vec{e}_\theta$$

The surface of the cone is regarded as being conductive. Therefore, the electrical field $\boldsymbol{E}$ is always perpendicular to it. With the geometry shown in Fig. 10 we have $\vec{\boldsymbol{E}}_P \| \vec{e}_\theta$ for all points P on the cone surface O. Hence:

$$\boldsymbol{E}_r = -\frac{\partial}{\partial r}\phi|_O = 0$$

$$\Rightarrow P_n(\cos\theta)|_O = 0 \qquad (12)$$

(see Eq. (11)). And therefore

$$\vec{\boldsymbol{E}}_P = -\phi_0 r^{n-1}\frac{\partial}{\partial\theta}P_n(\cos\theta)|_p\vec{e}_\theta \qquad \text{for all } P \in O$$

$$\Rightarrow p_E = \tfrac{1}{2}\epsilon_0\phi_0^2 r^{2(n-1)}\left[\frac{\partial}{\partial\theta}P_n(\cos\theta)\right]^2$$

(see Eq. (2)). This is the pressure caused by the electrostatic force.

5.3. The force on an elliptically shaped fluid surface

For an elliptically shaped fluid surface which approximates the shape of a Taylor Cone the following electrical potential is

assumed (see Fig. 4, Eq. (5)).

$$\phi(r,\theta) = \phi_0(r^{0.5} - a^2 r^{-1.5})P_{1/2}(\cos\theta)$$

The fluid surface O lies at the potential U_0 (see Fig. 4). So we have

$$U_0 = \phi(r_0, 0) = \phi_0(r_0^{0.5} - a^2 r_0^{-1.5})$$

$$\phi(r,\theta)|_P = \frac{U_0}{r_0^{1/2} - a^2 r_0^{-3/2}}$$

$$\times(r^{1/2} - a^2 r^{-3/2})P_{1/2}(\cos\theta) = U_0 \qquad (13)$$

for all points $P \in O$.

With the parameters $x = r/r_0$ and $k = a/r_0$ we get an expression describing the shape of the ellipsoid

$$P_{1/2}(\cos\theta) = \frac{1 - k^2}{x^{1/2} \cdot \left(1 - \frac{k^2}{x^2}\right)} \qquad (14)$$

With $k = 0.5$ the ellipsoid approaches the shape of the Taylor Cone [16].

During operation a certain voltage U_a is applied to the spray. This voltage corresponds to the difference between the values U_0 and U_1 in Fig. 4. The electrical potential can be chosen such that $U_a = \phi(r_1, 0)$. Then we have

$$E(r_0, 0) = E_r(r,\theta)|_P = -\frac{\partial}{\partial r}\phi(r,\theta)|_P$$

$$= 0.5\phi(r_1, 0)(r_1 r_0)^{-0.5}(1 + 3(a/r_0)^2)$$

(see Eq. (13)).

If the cone angle of the ellipsoid is near to the cone angle of a Taylor Cone a sphere of the radius r_a with $r_a = 7r_0$ approximates the shape of the ellipsoid at its apex point P as shown by computer calculations [16]. With $k = a/r_0$ we get for the electrical field at the apex of the fluid ellipsoid

$$E(r_0, 0) = 1.323U_a(r_a r_1)^{-0.5}(1 + 3k^2) = \mathrm{d}V_a \qquad (15)$$

Using Eqs. (1) and (2) we can calculate the conditions for the equilibrium between the electrostatic force and the surface tension at the apex point. The curvature for a sphere of the radius r_a is $2/r_a$ and therefore

$$p_\gamma - p_E = (1/r_a)$$

$$\times(2\gamma - 0.5\epsilon_0 U_a^2 1.323^2 r_1^{-1}(1 + 3k^2)^2) \qquad (16)$$

This equation describes the forces on the liquid surface when a voltage U_a is applied to the fluid. For $k = 0.5$ the shape of the ellipsoid approximates that of the Taylor Cone [16].

5.4. The correlation between the curvature r_a and the emission radius r_e

The emission radius for the droplets at the tip of a spraying Taylor Cone and the curvature of the fluid surface between the emission of two droplets as assumed in Fig. 5 are geometrically correlated. The tip is approximated by an ellipse which touches the Taylor Cone tangentially in the point P. The curvature at the apex r_a is $7r_0$ [16]. We have:

$$f(x) = (1 - x^2/a^2)^{0.5} b$$

$$g(x) = \tan\left(\frac{\pi}{2} - \vartheta\right)x + b + r_0$$

$$f''(0) = -r_a^{-1}$$

$$f'(r_e) = \tan\left(\frac{\pi}{2} - \vartheta\right)$$

$$z' = (1 - r_e^2/a^2)^{0.5} b$$

$$z' = \tan\left(\frac{\pi}{2} - \vartheta\right)r_e + b + r_0$$

From the last four equations we get an expression for r_e, the emission radius of droplets from the cone.

$$r_e = r_a \tan\left(\frac{\pi}{2} - \vartheta\right) \qquad (17)$$

5.5. The current/voltage characteristics

The $I-U$ characteristics of the spray will be calculated under the assumption that the surface density of the charge stays constant

throughout the experiment and that spheres with the radius r_e are emitted from the Taylor Cone.

$$q_{\text{droplet}}/S_{\text{droplet}} = c \Rightarrow I = c4\pi r_e^2 \, dn/dt$$

with q_{droplet} the charge on one droplet, S_{droplet} the surface of the droplet, c the surface charge density and $dn/dt = (dV/dt)/V_{\text{droplet}}$ the emission rate of droplets.

The flow rate dV/dt is determined by the pressure $p_E - p_\gamma$ which pulls the liquid out of the capillary and the overall flow resistance R_f.

$$dV/dt = (p_E - p_\gamma)/R_f$$

When substituting the pressure from Eq. (8) and the emission radius from Eq. (9) the current becomes:

$$I = 6\left(\frac{\pi^2}{\rho}\right)^{2/5} \frac{c}{R_f^{1/5}} \left[T \tan\left(\frac{\pi}{2} - \vartheta\right)\right]^{3/5} \times \left\{\left(\frac{U_a}{U_T}\right)^2 - 1\right\}^{3/5} \quad (18)$$

At the Rayleigh stability limit the surface charge density of a sphere with the radius r_e is $c = (16\epsilon_0\gamma/r_e)^{1/2}$ and therefore

$$I_{\max} = 12\pi T \left(\frac{\epsilon_0 \tan\left(\frac{\pi}{2} - \vartheta\right)}{\rho}\right)^{1/2} \times \left\{\left(\frac{U_a}{U_T}\right)^2 - 1\right\}^{1/2} \quad (19)$$

Acknowledgements

This work was done in partial fulfilment of the requirement for the Ph.D. degree (M.W.) at the University of Münster.

References

[1] M. Yamashita and J.B. Fenn, J. Phys. Chem., 88 (1984) 4451.
[2] M.L. Aleksandrov, L.N. Gall, V.N. Krasnov, V.I. Nikolaev, V.A. Pavlenko and V.A. Shkurov, Dokl. Akad. Nauk SSSR, 277 (1984) 379.
[3] M.L. Aleksandrov, L.N. Gall, V.N. Krasnov, V.I. Nilolaev, V.A. Pavlenko, V.A. Shkurov, G.I. Baram, M.A. Gracher, V.D. Knorre and Y.S. Kisner, Bioorg. Khim., 10 (1984) 710.
[4] M. Dole, L.L. Mack, R.L. Hines, R.C. Mobley, L.D. Ferguson and M.B. Alice, J. Chem. Phys, 49(5) (1968) 2240.
[5] S.F. Wong, C.K. Meng and J.B. Fenn, J. Phys. Chem., 92 (1988) 546.
[6] C.K. Meng, M. Mann and J.B. Fenn, Z. Phys. D. 10 (1988) 361.
[7] A.P. Bruins, T.R. Covey and J.D. Henion, Anal. Chem., 59 (1987) 2642.
[8] B.A. Thomson and J.V. Iribarne, J. Chem. Phys, 71, 11 (1979) 4451.
[9] J.B. Fenn, J. Am. Soc. Mass Spectrom. 4 (1993) 524.
[10] J.B. Fenn, M. Mann, C.K. Meng, S.F. Wong and C.M. Whitehouse, Mass Spectrom. Rev., 9 (1990) 37.
[11] F.W. Röllgen, E. Bramer-Weger and L. Bütfering, J. Phys., Colloq., 48 (1987) 253.
[12] R.D. Smith and K.J. Light-Wahl, Biol. Mass Spectrom., 22 (1993) 493.
[13] M. Mann, Org. Mass Spectrom., 25 (1990) 575.
[14] G. Taylor, Proc. R. Society London Ser. A, 280 (1964) 383.
[15] M. Wilm, ter Meer–Müller–Steinmeister & Partner, European Patent Attorneys, Artur-Ladebeckl-Str. 51, D-33 617 Bielefeld, File XW15 (1991).
The concept of micro electrospray was developed by M. Wilm in 1988/89 in the Department of Experimental Physics at the University of Münster Germany, in the group of Prof. Dr. A. Benninghoven.
[16] R. Gomer, Appl. Phys., 19 (1979) 365.
[17] J. Fernández de la Mora, J. Fluid Mech., 243 (1992) 561.
[18] S.P. Thompson and P.D. Prewett, J. Phys. D: Appl. Phys., 17 (1984) 2305.
[19] A. Gomez and K. Tang, Phys. Fluids, in press.
[20] P. Kebarle and L. Tang, Anal. Chem., 65, 22 (1993) 972.
[21] R.C. Weast and M.J. Astle (Eds.), CRC Handbook of Chemistry and Physics, 63rd edn., CRC Press, Boca Raton, FL, 1982–1983.
[22] D.C. Gale and R.D. Smith, Rapid Commun. Mass Spectrom., 7 (1993) 1017.